

Terahertz quartz enhanced photo-acoustic sensor

S. Borri, P. Patimisco, A. Sampaolo, H. E. Beere, D. A. Ritchie et al.

Citation: *Appl. Phys. Lett.* **103**, 021105 (2013); doi: 10.1063/1.4812438

View online: <http://dx.doi.org/10.1063/1.4812438>

View Table of Contents: <http://apl.aip.org/resource/1/APPLAB/v103/i2>

Published by the [AIP Publishing LLC](#).

Additional information on *Appl. Phys. Lett.*

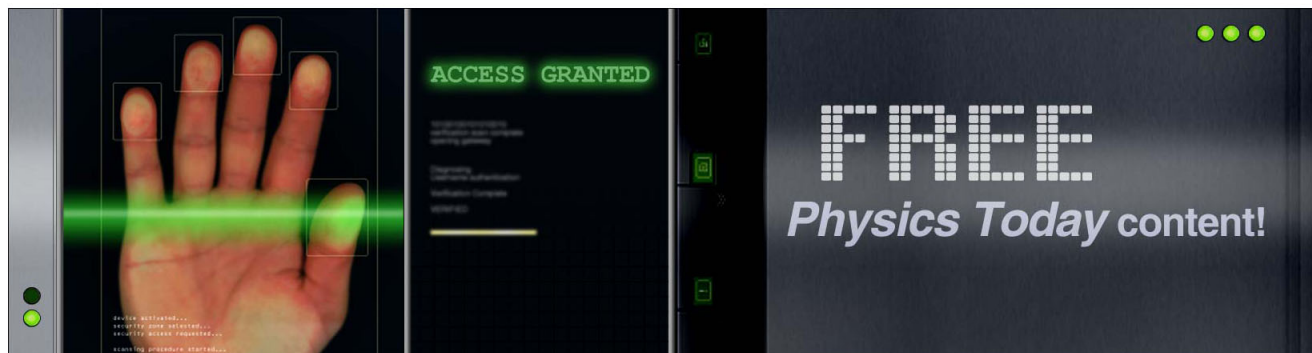
Journal Homepage: <http://apl.aip.org/>

Journal Information: http://apl.aip.org/about/about_the_journal

Top downloads: http://apl.aip.org/features/most_downloaded

Information for Authors: <http://apl.aip.org/authors>

ADVERTISEMENT



Terahertz quartz enhanced photo-acoustic sensor

S. Borri,¹ P. Patimisco,² A. Sampaolo,² H. E. Beere,³ D. A. Ritchie,³ M. S. Vitiello,⁴
 G. Scamarcio,^{1,2} and V. Spagnolo^{1,2,a)}

¹*IFN-CNR UOS Bari, via Amendola 173, 70126 Bari, Italy*

²*Dipartimento Interateneo di Fisica, Università e Politecnico di Bari, Via Amendola 173, 70126 Bari, Italy*

³*Cavendish Laboratory, University of Cambridge, J. J. Thomson Avenue, Cambridge CB3 0HE, United Kingdom*

⁴*NEST, CNR - Istituto Nanoscienze and Scuola Normale Superiore, Piazza San Silvestro 12, 56127 Pisa, Italy*

(Received 25 March 2013; accepted 8 May 2013; published online 8 July 2013)

A quartz enhanced photo-acoustic sensor employing a single-mode quantum cascade laser emitting at 3.93 Terahertz (THz) is reported. A custom tuning fork with a 1 mm spatial separation between the prongs allows the focusing of the THz laser beam between them, while preventing the prongs illumination. A methanol transition with line-strength of 4.28×10^{-21} cm has been selected as target spectroscopic line. At a laser optical power of $\sim 40 \mu\text{W}$, we reach a sensitivity of 7 parts per million in 4s integration time, corresponding to a 1σ normalized noise-equivalent absorption of $2 \times 10^{-10} \text{ cm}^{-1}\text{W/Hz}^{1/2}$. © 2013 AIP Publishing LLC. [<http://dx.doi.org/10.1063/1.4812438>]

Recent technological innovation in photonics and nano-technology is now enabling Terahertz (THz) research to be applied in an increasingly wide variety of applications, such as information and communications technology, medical sciences, global environmental monitoring, homeland security, quality and process controls. Most of the above applications involve the use of THz spectroscopic systems. Explosives, narcotics, and toxic gases (i.e., carbon monoxide, hydrogen cyanide, hydrogen chloride and methanol) have indeed distinct spectral “fingerprints” and strong absorption bands across the THz range.

To address the above application requirements, suitable sensing systems equipped with high power, widely tunable sources, and high speed, high sensitivity detectors have to be developed. To date, only a few systems have been successfully demonstrated to operate across the far-infrared. Photomixing-based sensors in the 0.5–1.5 THz range have been recently proposed¹ for detection of HCN, CO, H₂CO, reaching sensitivities of 9 parts per million in volume (ppm), 0.1% and 114 ppm, respectively. Broadband OCS, N₂O, and CH₃OH sensors at 0.5 THz, based on chirped-pulse THz absorption spectroscopy, have been also demonstrated, reaching noise equivalent concentration of a few hundreds ppm.² Methyl chloride detection in the ppm range with long-baseline THz spectroscopy based on a White cell design has been also reported.³

The described systems suffer from the low power levels of the employed THz sources and/or the low sensitivity of the detection units. THz quantum cascade lasers (QCLs) can offer a significant improvement in terms of compactness and sensitivity levels, stemming from the single-mode high spectral purity emission,⁴ the relatively broad tunability range (up to 10% of the central frequency),⁵ the high continuous wave (CW) output power levels (up to 138 mW),⁶ and the relatively good compactness provided by Stirling cryocooler systems. THz QCLs have indeed recently demonstrated interesting performance in high resolution molecular

spectroscopies, in both direct absorption^{7–10} or wavelength modulation spectroscopy,¹¹ showing a minimum detectable absorption α_{min} in the $10^{-6} \text{ cm}^{-1}\text{Hz}^{-1/2}$ range, mostly thanks to the employed sensitive cryogenic detectors. Improving such detection sensitivities requires either switching to novel low noise equivalent power (NEP) room temperature nano-detectors,^{12,13} or moving to alternative high performance spectroscopic techniques.

Quartz-enhanced photo-acoustic spectroscopy (QEPAS) showed high sensitivity, fast time-response and high compactness in the near-IR and mid-IR spectral ranges. The distinguishing feature of QEPAS is the use of a low loss quartz tuning fork (QTF) for detection of the optically generated sound.¹⁴ Very efficient mid-IR QCL-based QEPAS sensors have been recently demonstrated for trace detection of several chemical gas species,^{14–17} with a record normalized noise-equivalent absorption (NNEA) sensitivity of $2.7 \times 10^{-10} \text{ W}\cdot\text{cm}^{-1}\cdot\text{Hz}^{-1/2}$ (1σ) for SF₆,¹⁸ corresponding to an α_{min} of $1.5 \times 10^{-8} \text{ cm}^{-1}\text{Hz}^{-1/2}$ and a detection limit of 50 parts per trillion (ppt) in 1 s. One of the main advantages of the photoacoustic spectroscopy techniques is that no optical detection is required.¹⁹ Thus, the extension of the QEPAS technique in the THz range would allow to avoid the use of low-noise but expensive, bulky, and cryogenic bolometers.

Standard QTFs have resonance frequencies of ~ 32.7 kHz and are characterized by a very small sensitive volume between its prongs ($\sim 0.3 \times 0.3 \times 3 \text{ mm}^3$). In QEPAS experiments, it is critical to avoid laser illumination of the QTF, since the radiation blocked by the QTF prongs results in an undesirable non-zero background. This background can be several times larger than the thermal noise level of QEPAS and carries a shifting fringe-like interference pattern, which strongly limit the sensor detection sensitivity.^{18,20} The reduced space (300 μm) between the QTF prongs, comparable with the wavelength of THz sources, so far has represented the main limitation preventing the use of QEPAS system in THz range. Larger size QTFs are, therefore, mandatory to operate in the THz range.

In this paper, we report on the development of a THz QEPAS sensor employing a 3.93 THz QCL and custom-made

^{a)}Electronic mail: vincenzo.spagnolo@uniba.it

QTF. Standard photolithographic techniques were used to etch the custom QTF, starting from z-cut quartz wafer. Chromium/gold contacts were deposited on both sides of the QTF. The overall QTF dimension was $3.3\text{ cm} \times 0.4\text{ cm} \times 0.8\text{ cm}$; each prong was 2.0 cm long and 2.5 mm wide. The gap between the prongs was $\sim 1\text{ mm}$. The QTF first flexion resonance falls at $f_0 \sim 4246\text{ Hz}$, in agreement with previous studies reported for a similar QTF.²¹ At atmospheric pressure we measured a Q factor of 9930. For our QEPAS THz sensor demonstration we selected methanol as target gas molecule. Methanol is widely used as a solvent, detergent, or even denaturant additive for industrial ethanol, and its ingestion can be fatal due to its toxication.

A scheme of the employed experimental system is shown in Fig. 1.

A single-mode $250\text{ }\mu\text{m}$ wide, 1.5 mm long bound-to-continuum Fabry-Perot QCL fabricated in a single plasmon configuration and emitting at 3.93 THz ($76.3\text{ }\mu\text{m}$) (Ref. 22) was mounted on the cold finger of a continuous-flow cryostat equipped with polymethylpentene (TPX) windows ($\sim 70\%$ transmission) and kept at a heat sink temperature of 6 K , while driven in CW mode. Despite the few hundreds Hz intrinsic linewidth,⁴ due to temperature and electrical bias fluctuations the free running linewidth exceeds 1 MHz over few seconds time scale.²³

By using a calibrated pyroelectric power meter, we measured a CW output power of $180\text{ }\mu\text{W}$ at 770 mA injected current. The THz beam was collimated using a 2 in. diameter ($f/\# = 1$) 90° off-axis paraboloidal reflector and focused by a second reflector (2 in. diameter, $f/\# = 3$) between the two prongs of the tuning fork, housed in a acoustic detection module (ADM) with TPX input and output windows. We achieved a focused beam waist radius of $\sim 240\text{ }\mu\text{m}$, as measured with a pyroelectric camera. By measuring the radiation power transmitted through the QTF using a pyroelectric detector, we verified that $\sim 100\%$ of the incoming laser beam was transmitted through the prongs without hitting the QTF.

QEPAS experiments were performed by applying a sinusoidal modulation to the QCL current at the QTF resonance frequency f_0 , while detecting the QTF response at the same frequency by means of a lock-in amplifier. QEPAS spectral measurements were performed by slowly scanning the laser

wavelength over $\sim 0.025\text{ cm}^{-1}$, applying a low-frequency (10 mHz) voltage ramp to the external analog modulation input of the current supply (ILX-LDX 3232, bandwidth $0\text{ Hz} - 250\text{ kHz}$). By means of a power combiner (DC to 12 GHz), the sinusoidal dither at f_0 is added to the low-frequency voltage ramp, to obtain up to 0.01 cm^{-1} optical frequency modulation. QEPAS measurement in locked-mode was performed by keeping fixed the laser wavelength on the absorption peak frequency and modulating its current at f_0 . The lock-in amplifiers and a function generator (Tektronix model AFG3102) are controlled through a universal serial bus National Instruments card, respectively, using LABVIEW-based software. The piezoelectric signal generated by the QTF is amplified by a custom transimpedance amplifier (feedback resistor $R_{fb} = 10\text{ M}\Omega$, gain = 30). The control electronics unit (CEU) is used to determine the QTF parameters: dynamic resistance R , Q-factor, and f_0 . Unless differently specified, the lock-in time constant was set to 50 ms , corresponding to a bandwidth of 3.335 Hz .

To test our sensor, we selected methanol. In the laser emission range methanol exhibits a rotational absorption line falling at 131.054 cm^{-1} ($v = 1, K = 6, J = 11$) $\leftarrow (1, 5, 10)$ with line-strength $S = 4.28 \times 10^{-21}\text{ cm/molecule}$, about two orders of magnitude stronger than that of the nearby methanol absorption lines.^{24,25} Thus, we performed direct absorption spectroscopic measurements (using a 14 cm -long cell filled with pure methanol at 2 Torr) and, as expected, we observed a main absorption line. The line-strength extracted from absorption measurements was in good agreement with the expected one. So in our QEPAS experiments we exploit the absorption measurement to fine tune the laser frequency on the selected methanol absorption line at 131.054 cm^{-1} .

Gas mixtures with different methanol concentrations have been obtained by diluting methanol vapors, collected from a reservoir held at the vapor pressure ($\sim 120\text{ Torr}$ at 300 K), with pressurized N_2 . For measurements at low concentrations, we used a certified 100 ppm methanol/ N_2 gas mixture. Preliminary measurements were performed to determine the best operating conditions in terms of QEPAS signal-to-noise, as a function of gas pressure, laser current modulation depth and resonance frequency. Note that the possibility to use a lower resonance frequency with respect to standard QTF, partially relaxes the gas excess energy relaxation time requirements and allows to work at low pressures, taking advantages of the corresponding larger Q factors. The best operating conditions have been observed at 10 Torr pressure and 600 mV peak-to-peak modulation voltage. Under these conditions, the physical parameters of the QTF, using N_2 as gas carrier, were $Q = 76300$, $f_0 = 4246.73\text{ Hz}$, and $R = 6.5\text{ M}\Omega$. From these data, we extracted a QTF thermal noise of $0.12\text{ }\mu\text{V}$, about one order of magnitude smaller than that typically observed for standard QTFs.^{15,18}

A representative spectral scan of 0.75% methanol in N_2 gas mixture is shown in Fig. 2(a). With a pressure broadening coefficient of 10 MHz/Torr (7.4 MHz/millibar) (Ref. 26) the expected line-width is $\sim 100\text{ MHz}$ (half width at half maximum, HWHM), with a negligible Doppler contribution (4.5 MHz HWHM). We used this estimate to convert the horizontal scale from time to frequency span (MHz). Note that the laser linewidth is much lower than the spectral line width of the methanol absorption feature. On the same energy

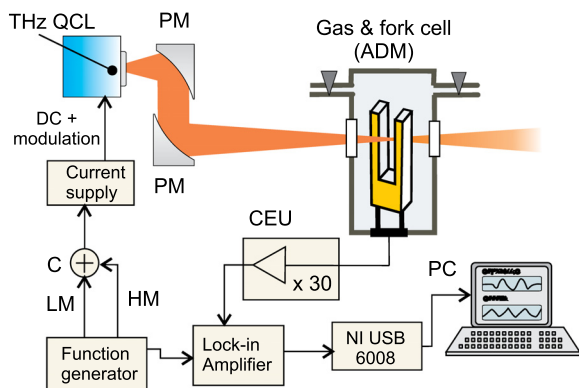


FIG. 1. Schematic of THz QCL-based QEPAS sensor. PM—paraboloidal mirror; C—power combiner; LM, HM—low-frequency modulation (triangular ramp), high-frequency modulation; CEU—control electronics unit; PC—personal computer.

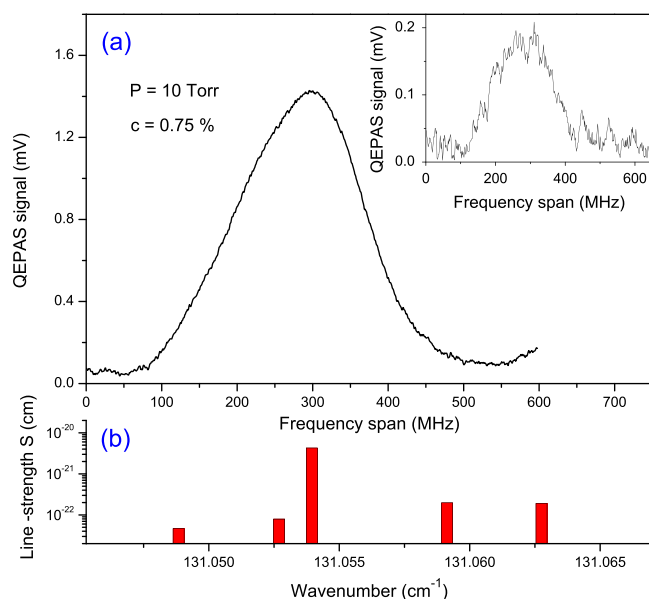


FIG. 2. (a) Spectral scan of 0.75% methanol in N_2 at $P = 10$ Torr, acquired with a modulation depth of 12 mA (~ 100 MHz) and 500 ms integration time. Inset: QEPAS acquisition of a methanol/ N_2 sample with a certified concentration of 100 ppm and lock-in integration time of 3 sec. The noise fluctuations are $\sim \pm 25 \mu V$. (b) Line strengths of the main methanol transitions (vertical bars), as reported in the JPL database,²⁵ falling in the energy range corresponding to the frequency span of Fig. 2(a).

span, in Fig. 2(b) are reported the line-strengths of the main methanol transitions (vertical bars), as tabulated in the Jet Propulsion Laboratory (JPL) database.²⁵ In the inset of Fig. 2(a) is shown a QEPAS spectral scan obtained for a certified 100 ppm methanol in N_2 gas mixture, using a 3 s lock-in integration time. Considering the noise fluctuations $\pm 25 \mu V$ and the QEPAS peak signal for 100 ppm methanol concentration ($\sim 170 \mu V$), we can extract for our THz QEPAS sensor a 1σ detection limit of ~ 15 ppm at 3 s integration time.

Stepwise concentration measurements were performed to verify the linearity of the QEPAS signal as a function

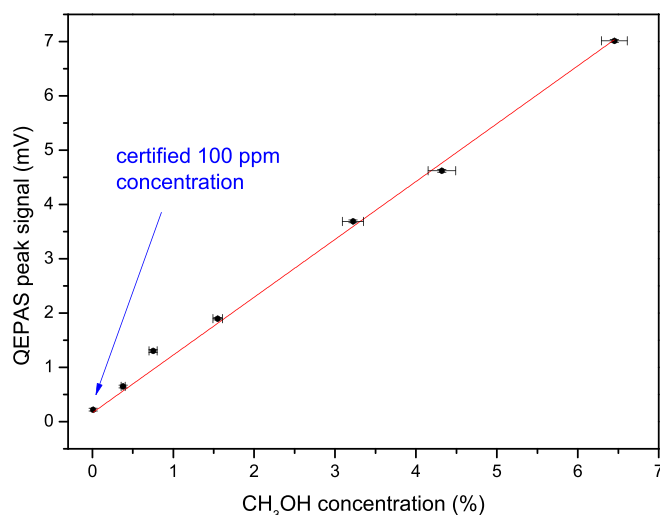


FIG. 3. Mean value of the QEPAS peak signals measured for gas mixture samples with different methanol concentrations in locked mode at 10 Torr pressure. The red line is a linear fit of the data ($R^2 = 0.9963$). The small deviations from the linear trend are partially due to uncertainty in the gas mixture concentration.

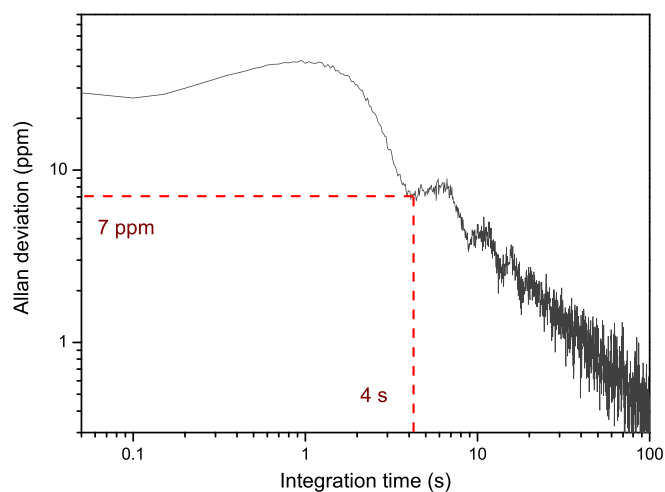


FIG. 4. Allan deviation in ppm of the QEPAS signal as a function of the integration time. The initial growth from 0.1 to 1 s reflects delays due to the signal sampling time (200 ms). The oscillations at integration time larger than 4 s are due to slow mechanical drifts of the ADM mounting.

of the methanol concentration. The system was operated in the locked mode, i.e., with the QCL frequency set to the center of the absorption line. Under this condition an optical laser power of $40 \mu W$ is focused on the QTF. In Fig. 3, the mean value of the QEPAS peak signal is plotted for different methanol concentrations from 6.5% down to 0.01% (100 ppm). The associated error bars take into account both the QEPAS signal fluctuations (standard deviation) and the uncertainty on the methanol concentration (uncertainty on the reading of the pressure gauge of ± 0.2 Torr). The experimental data show the expected linear dependence of the QEPAS signal from the methanol concentration.

In order to determine the best achievable sensitivity of the QEPAS sensor we performed an Allan variance analysis measuring and averaging the QEPAS signal at zero methanol concentration (pure N_2). The obtained Allan deviation in ppm is shown in Fig. 4. For a 4 sec averaging time (i.e., 0.04 Hz bandwidth), we achieve a detection sensitivity of 7 ppm, corresponding to a minimum absorption coefficient $\alpha_{\min} = 9.5 \times 10^{-7} \text{ cm}^{-1}$ (laser power of $\sim 40 \mu W$). The calculated NNEA is $2 \times 10^{-10} \text{ cm}^{-1} \text{ W}/\text{Hz}^{1/2}$ (1σ), comparable with the best result obtained in the mid-IR¹⁸ and at least one order of magnitude better than those obtainable with room-temperature pyroelectric detectors and in strong competition with the sensitivities achieved with the most sensitive cryogenic bolometers.

In conclusion, we extend the possibility to employ the QEPAS technique in the THz spectral range, using a THz QCL source and a custom QTF. The simple apparatus architecture and the independence of the detection unit from the laser frequency make the proposed sensor highly versatile in the spectral domain actually accessible to THz QCLs. In addition, the possibility to employ high power CW (~ 100 mW) THz QCLs for the detection of strong THz absorbing molecules like OH or HF, having line-strengths of the order of 10^{-18} cm , would allow QEPAS detection sensitivity in the few parts per trillion concentration range. Furthermore, the possibility to implement compact QEPAS

THz systems, with no optical detector needed, based on portable closed-cycle Stirling cryo-cooler opens the way to the use of THz sensor systems for in-situ security and environmental monitoring.

The authors acknowledge financial support from the Italian national projects: PON01_02238 and PON02_00675. We thank A. Tredicucci for fruitful interactions, F. Tittel for helpful discussions, A. Kachanov for providing the 4.25 kHz quartz tuning fork, and P. P. Calabrese for realizing the fork housing. M.S.V. acknowledges financial support of the Italian Ministry of Education, University, and Research (MIUR) through the program “FIRB-Futuro in Ricerca 2010” RBFR10LULP “Fundamental research on terahertz photonic devices”

- ¹D. Bigourd, A. Cuisset, F. Hindle, S. Matton, R. Bocquet, G. Mouret, F. Cazier, D. Dewaele, and H. Nouali, *Appl. Phys. B* **86**, 579 (2007).
²E. Gerecht, K. O. Douglass, and D. F. Plusquellic, *Opt. Express* **19**, 8973 (2011).
³S. A. Harmon and R. A. Chevillea, *Appl. Phys. Lett.* **85**, 2128 (2004).
⁴M. S. Vitiello, L. Consolino, S. Bartalini, A. Taschin, A. Tredicucci, M. Inguscio, and P. De Natale, *Nature Photon.* **6**, 525 (2012).
⁵M. S. Vitiello and A. Tredicucci, *IEEE Trans. Terahertz Sci. Technol.* **1**, 76 (2011).
⁶B. S. Williams, S. Kumar, Q. Hu, and J. L. Reno, *Electron. Lett.* **42**, 89 (2006).
⁷H. W. Hübers, S. G. Pavlov, H. Richter, A. D. Semenov, L. Mahler, A. Tredicucci, H. E. Beere, and D. A. Ritchie, *Appl. Phys. Lett.* **89**, 061115 (2006).
⁸H. W. Hübers, S. G. Pavlov, H. Richter, A. D. Semenov, L. Mahler, A. Tredicucci, H. E. Beere, and D. A. Ritchie, *J. Nanoelectron. Optoelectron.* **2**, 101 (2007).
⁹H. W. Hübers, M. F. Kimmitt, N. Hiromoto, and E. Brundermann, *IEEE Trans. Terahertz Sci. Technol.* **1**, 321 (2011).

- ¹⁰Y. Ren, D. J. Hayton, J. N. Hovenier, M. Cui, J. R. Gao, T. M. Klapwijk, S. C. Shi, T.-Y. Kao, Q. Hu, and J. L. Reno, *Appl. Phys. Lett.* **101**, 101111 (2012).
¹¹L. Consolino, S. Bartalini, H. E. Beere, D. A. Ritchie, M. S. Vitiello, and P. De Natale, *Sensors* **13**, 3331 (2013).
¹²M. S. Vitiello, D. Coquillat, L. Viti, D. Ercolani, F. Teppe, A. Pitanti, F. Beltram, L. Sorba, W. Knap, and A. Tredicucci, *Nano Lett.* **12**, 96 (2012).
¹³L. Vicarelli, M. S. Vitiello, D. Coquillat, A. Lombardo, A. C. Ferrari, W. Knap, M. Polini, V. Pellegrini, and A. Tredicucci, *Nature Mater.* **11**, 865 (2012).
¹⁴A. A. Kosterev, F. K. Tittel, D. V. Serebryakov, A. L. Malinovsky, and I. V. Morozov, *Rev. Sci. Instrum.* **76**, 043105 (2005).
¹⁵L. Dong, A. A. Kosterev, D. Thomazy, and F. K. Tittel, *Appl. Phys. B* **100**, 627 (2010).
¹⁶K. Liu, H. Yi, A. A. Kosterev, W. Chen, L. Dong, L. Wang, T. Tan, W. Zhang, F. K. Tittel, and X. Gao, *Rev. Sci. Instrum.* **81**, 103103 (2010).
¹⁷L. Dong, V. Spagnolo, R. Lewicki, and F. K. Tittel, *Opt. Express* **19**, 24037 (2011).
¹⁸V. Spagnolo, P. Patimisco, S. Borri, G. Scamarcio, B. E. Bernacki, and J. Kriesel, *Opt. Lett.* **37**, 4461 (2012).
¹⁹A. Elia, P. M. Lugarà, C. Di Franco, and V. Spagnolo, *Sensors* **9**, 9616 (2009).
²⁰V. Spagnolo, A. A. Kosterev, L. Dong, R. Lewicki, and F. K. Tittel, *Appl. Phys. B* **100**, 125 (2010).
²¹N. Petra, J. Zwick, A. A. Kosterev, S. E. Minkoff, and D. Thomazy, *Appl. Phys. B* **94**, 673 (2009).
²²T. Losco, J. H. Xu, R. P. Green, A. Tredicucci, H. E. Beere, and D. A. Ritchie, *Physica E* **40**, 2207 (2008).
²³A. Barkan, F. K. Tittel, D. M. Mittleman, R. Dengler, P. H. Siegel, G. Scalari, L. Ajili, J. Faist, H. E. Beere, E. H. Linfield, A. G. Davies, and D. A. Ritchie, *Opt. Lett.* **29**, 575 (2004).
²⁴G. Moruzzi, P. Riminucci, F. Strumia, B. Carli, M. Carlotti, R. M. Lees, I. Mukhopadhyay, J. W. C. Johns, B. P. Winnewisser, and M. Winnewisser, *J. Mol. Spectrosc.* **144**, 139 (1990).
²⁵H. M. Pickett, R. L. Poynter, E. A. Cohen, M. L. Delitsky, J. C. Pearson, and H. S. P. Muller, “Submillimeter, millimeter, and microwave spectral line catalog,” *J. Quant. Spectrosc. Radiat. Transf.* **60**, 883 (1998).
²⁶Y. Ren, J. N. Hovenier, R. Higgins, J. R. Gao, T. M. Klapwijk, S. C. Shi, A. Bell, B. Klein, B. S. Williams, S. Kumar, Q. Hu, and J. L. Reno, *Appl. Phys. Lett.* **97**, 161105 (2010).